Chapter 1

Introduction

1.1 Background and overview of OTFTs

In 2000, the Nobel Prize in chemistry was awarded for the development of conducting polymers. After Shirakawa began the research on the conducting property of polymers in late 1970s [1], the first demonstration of organic thin-film transistors (OTFTs) based on polyacetylene was reported in 1983 [2], but the mobility was quite low, on the order of 10^{-5}cm^2/Vs. The conductivity of the polymer can be altered from insulator to conductor through the method of doping. Consequently, the possibility of fabricating OTFTs with small conjugated molecules was shown in 1989 [3] with sex thiophene rings linked at alpha positions, showed mobility on the order of 10^{-1}cm^2/Vs, which has reached the display-requirement and is comparable to the amorphous-Si TFTs. The comparisons between amorphous-Si TFTs, poly-Si TFTs and OTFTs are listed in Table1.1 [4].

Nowadays, a large number of conjugated molecules and polymers have been used to be the active layers of OTFTs. The most significant difference between distinguishing those devices fabrication is the deposition method. Organic semiconductors are potentially solvable in organic solvent and are compatible to

deposit at low-temperature on plastic substrates. By the low-cost fabrication techniques such as spin-coating and inkjet-printing, OTFTs may be used in the applications of flexibility, large-area coverage without complex process system and saving more energy on green earth.

Since organic semiconductors can be processed at low temperatures and compatible with plastic substrates. Such applications include active-matrix liquid crystal displays (AMLCDs), active-matrix organic light-emitting diodes (AMOLEDs), and electronic paper displays. Additionally, organic sensors, organic solar cells, low-end smart cards, radio-frequency identification (RFID) tags, and other electronics integrated with organic circuits have been proposed.

The bonding between organic semiconductors is by van der Waals forces between the hydrogen atoms, which are dangling on the ends of the benzene rings. It is much weaker than that of the covalent force in inorganic materials, which is the reason for small mobility. In Fig. 1.1 [5], we can compare the increase of mobility in the past years for different organic semiconductors. If we want to overcome the materials limitation, there are several points we have to overcome. First, the injection from the contact electrodes to organic film must be optimized. Second, deposition conditions should be optimized to get the best molecular ordering. And third, the synthesis-technology will provide more opportunities for choosing new

organic semiconductor.

As shown in Fig. 1.2 [6], the current topics on OTFTs are still focused on p-type semiconductors, the development of n-type semiconductors is expected and under investigation.   The reliability and reproducibility are also important issues.   There is still room for further improvement, and the choices of materials for the electrodes [7], the insulator [8], the passivations [9], and the substrates [10] are also important factor.

1.1-1 Introduction to organic materials and pentacene

Organic conjugated materials used in OTFTs can be generally divided into two groups.   All exhibit contiguous sequences of double bonds separated by one single bond.   The π-orbital in the conjugated system is linked with the neighboring π orbital, and spreads in the whole molecule.   The π electrons are delocalized across the molecule, which makes semi-conductive or conductive characteristics in the conjugated system.   Unlike the case in inorganic semiconductors, the carrier transport is band-like transport which is determined by the Bloch wave states.   The carriers are hopping between the localized states in the disordered organic semiconductors.   The localized wave functions in organic semiconductors lead to small inter-molecular interactions；   typically the van der Waals or weak π-π overlap orbits-ping.   That is the main cause of the low mobility in organic materials. But it

can be improved by modifying the materials and device architectures.

Among the semiconductors, one group is the polymers and the other is the oligomers. The polymers are formed by a repeating chain of hydrogen and carbon in various configurations with other elements, but they have relatively poor mobilities (4×10^{-2} cm2/Vs [11]). The oligomers are held together by weak Van der Waal forces and thermal-evaporated with good ordering. Devices fabricated with oligomers have higher mobilities (1.5 cm2/Vs [12]).

Pentacene is one of the popular materials in OTFTs. Its mobility has reached the fundamental limit (>3cm^2/Vs) [13, 14] which is obtained with a single crystaline at room temperature. The mobility of pentacene is comparable to that of amorphous silicon which is widely developed and used in active matrix liquid crystal displays (AMLCD) and the other electronic applications.

Pentacene is an aromatic compound with five condensed benzene rings and therefore, the chemical formula is $C_{22}H_{14}$ with molecular weight 278.3. The volume of the unit cell is about 705Å [13]. The permittivity is 4 [14], and the electron affinity is about 2.49eV. Silinish et al. determined the adiabatic energy gap (E_G^{Ad}) by using the threshold function of intrinsic photoconductivity in pentacene [7]. The second transition is from the excited state to the ionic state, which is called the optical energy gap (E_G^{Opt}). According to Fig. 1.3, the adiabatic energy gap as 2.47eV and

the optical energy gap as 2.83eV is recorded [15].

1.1-2 Pentacene deposition and Contact issues

Pentacene is used as an active layer. Its purity leads to longer diffusion length for the charge transporting with less interaction with the lattice. Furthermore, the impurities in the material tend to chemically combine with the organic semiconductor material which leads to irregularities in the band gap [16]. Therefore, the thermal evaporation is carried out under high or ultra high vacuum conditions to avoid the impurities and increase the quality of the material.

It is well known that the deposition temperature, deposition pressure, and deposition rate are the three critical parameters to the organic film quality. Lower deposition rate and appropriate deposition temperature is expected to result in better ordering of the organic molecules, thin-film phase formation of pentacene film, and the better performance [17].

Then OTFTs are mainly bottom gate structure, the dielectrics is important. The roughness has a influence on the morphology, whereas the films on the smooth thermal oxide are in generally highly ordered. The surface chemistry also is a typical issue to organic devices. Changing surface wettability as a hydrophobic surface by surface treatment leads to mobilities increasing [18].

Contact configurations are divided into top-contact and bottom contact as

electrode formation after pentacene deposition or before it. The injection barrier of the OTFT device is determined by the affinity of the source and drain electrodes. Materials with large work function are preferred to form an Ohmic-contact. Metal with low work function is a schottky-like contact with organic film.

In the bottom-contact, the pentacene grain size on Au is dramatically reduced comparing to pentacene on oxide. Close to the Au edge and the SiO2 side is a transition region where the grain size is altered. In Fig. 1.4, it is the morphology of the pentacene film in the OTFT channel region close to the electrode edge that causes the performance degradation of the bottom contact OTFTs [19].

In top contact, pentacene morphology is not affected by the top metal. The disadvantage in bottom contact is not existed. The metal film formation of gold on a pentacene layer show signs of metal penetration coupled with formation of metal clusters in XPS and UPS studies [20,21], leading to a substantial reduction of the dipole barrier from 1.0 to 0.3eV. However, we note that the top contact architecture presents a major drawback: patterning the device through conventional micro-lithography is no longer achievable.

1.2 Operation of OTFTs

In the past few years, the major OTFTs structure of an organic transistor is top-contact or bottom-contact.   They are well-developed structures in thin-film transistors; therefore they seem to be the most standard structure of the organic transistor.   However, there are several subjects for using these devices structures. For example, top contact OTFT gives high performance efficiency due to the good affinity between organic layer and electrodes.   Though the process via shadow mask is easy to prepare, top-contact devices via lithography should damage the organic film. On the other hand, for the OTFT with bottom contact, it is easier to prepare the source and drain electrodes in smaller scales than the top-contact.   However, its performance seems to be poor owing to the non-optimized contact between the organic film and the electrodes.   It has been shown that the top-contact devices yield mobilities that are typically larger by a factor of two compared to bottom contact devices [22-24].   It is likely that there is still another structure for the OTFTs [7-11].

In top contact and bottom-contact OTFTs, both the general operation concept (e.g. p-type pentacene OTFTs) comes from inorganic transistors.   The MOSFET is traditionally operated in inversion mode.   However, the operation of OTFTs is generally in accumulation mode.   The typical I-V characteristics can be used to calculate the important parameters such as mobility, threshold voltage, and on/off

current ratio.

Pentacene is a p-type semiconductor. At first, a negative bias is applied to the gate, the voltage drops over the insulator region and semiconductor one, which gives rise to bend the band in the semiconductor. The additional positive charges provided from the source and drain electrodes will accumulate in this region. The insulator serves as a capacitance which stores charges and can be represented as C_{OX}. It is assumed that a little voltage drop across the semiconductor is negligible. In this situation, the applied drain-bias can force the current from the source to drain. The conduction is determined by mobility μ, which represents how the electrical field drives the accumulated charges. Therefore, the increased in gate voltage δV_G accounts for the increased charges $C_{OX}\delta V_G$ and the total charges induced over the channel are $WLC_{OX}\delta V_G$, where W and L correspond to the channel width and length. The increased drain current δI_D is then represented as

$$\delta I_D \approx \frac{W}{L}\mu C_{OX}V_D\delta V_G \tag{1.1}$$

In general, we can divide the operation of OTFTs into two regions, linear and saturation regions. The drain current in the linear region is determined from the following equation

$$I_D = \frac{W}{L}C_{OX}\mu(V_G - V_{TH} - \frac{V_D}{2})V_D \tag{1.2}$$

Since the drain voltage is quite small, sometimes equation (1.2) can be simplified as

$$I_D = \frac{W}{L} C_{OX} \mu (V_G - V_{TH}) V_D \qquad\qquad (1.3)$$

For $-V_D > -(V_G - V_{TH})$, I_D tends to saturate due to the pinch-off of the

accumulation layer.   The current equation is modified as

$$I_D = \frac{W}{2L} C_{OX} \mu (V_G - V_{TH})^2 \qquad\qquad (1.4)$$

The energy band diagrams for p-type and n-type OTFT are shown in Fig. 1.5. [25]

1.3 Motivation

For the practical applications, the output current is still the main issue for the OTFTs.   Among the mentioned issues, if we want to enhance the OTFT performance. Reducing the transistor channel-length may be effective [26].   With the high resolution lithography systems, such as G-Line, I-Line photolithography system, or the e-beam direct writer system, the organic devices with nano-scale channel length are realized fulfilled [27]-[29].   In these processes, OTFTs will require the high-cost instrument and are hard to utilize in large-area fabrication.

In this study, a simple and low-cost way to reduce the channel length is proposed. We demonstrated two structures, without the complex process flow or high-resolution lithography system.   For OTFTs, the sub-micron channel length and the asymmetric electrodes are achieved by using only the shadow mask and simple aligner.   The first structure is Vertical OTFT (VOTFT).   In the conventional OTFTs, the channel length is in the order of about several μm.   Since the organic film is in the order of nano meter, we re-configured the electrodes vertically and capped the electrodes (source and drain) on both sides of organic film.   The vertical-electrodes could guide the current perpendicularly and the channel length will be determined by the organic film thickness.   The channel length could be significantly reduced without high-resolution lithography system.   The second is TBC (Top-Bottom Contact)

OTFTs.   TBC-OTFTs can be regarded as a kind of VOTFT but the source and drain

electrodes are not overlapped.   The top and bottom electrodes were all deposited

through the shadow masks; further lowered the fabrication cost.

1.4 Organization of this thesis

In Chapter 1, we described the background, development, brief overview and motivation of this study.   In Chapter 2, the devices fabrication, measurement and parameter extraction of OTFTs are presented.   In Chapter 3, different structures are investigated and discussed. Finally, we will provide a conclusion in Chapter 4.

Chapter 2

Experiment Methods

2.1 Device structures and fabrication

2.1-1 Vertical OTFT

Step1. Substrate and gate electrode

4-inch n-type heavily-doped single crystal silicon wafer (100) is used as the substrate and the gate electrode.

Step2. Gate oxide formation

After the initial RCA cleaning, the 1000Å thermally grown SiO_2 layer is deposited in furnace.

Step3. Source definition

Bi-layer metals (Pd/Ti) were deposited as source electrode by the E-gun deposition system (ULVAC EBX-10C). The deposition pressure was at 3×10^{-6}torr with the deposition rate of 0.5~1Å/sec. The thicknesses of the Pd and Ti layers were 1000Å and 10Å, respectively. Pd from a better injection with active layer and Ti is a adhesion layer to Pd on oxide.

After the formation of the Pd/Ti layers, the source electrode is defined by photolithography. The photoresist FH-6400 is spin-coated with 1000rpm for 10 seconds followed by 4000rpm for 40 seconds and then soft-baked at 90°C for 1 minute. The exposure energy and exposure time are 300W and 50seconds. And then, the device is developed by FHD-5. After rinsed with water, hard bake of 3 minutes at 120°C is used to expel the solvent inside the photoresist. After pattern definition, the Pd/Ti layers are etched by aqua regia (HNO_3:HCl:$H_2$0=1:3:4 at temperature $>70^{\circ}$C). Finally, photoresist is stripped by acetone.

Step4. Pentacene film deposition through shadow mask

Pentacene, which was obtained form Aldrich Chemical Company without any purification, was used as an active layer. The deposition is started at a pressure lower than 3×10^{-6}torr. The deposition rate is controlled at 0.5Å/s. The temperature we use in depositing pentacene films is 70 ^{o}C. We use shadow mask to define the active region of each device.

.

Step5. Drain formation (Au deposition for Top Contact)

We use shadow mask to define top contact of each device. The top electrodes are Au. As illustrated in Fig. 2.2, we deposited the Au (500Å) via the thermal evaporator as the drain electrode pad. The deposition pressure was at 3×10^{-6}torr with the

deposition rate of 0.5~1Å/sec. Several individual drain electrodes were formed on the pentacene film. Some of the drain electrodes are vertically overlapped with the window-like source electrodes, they are clarified to be electrode A as shown in Fig. 2.3. Some of the drain electrodes (ex. electrode B in Fig. 2.1) are not overlapped with the source electrode.

The top view image that captured from the microscope CCD was showed in figure 2.2. The configuration of electrode pad and the active region could be clearly observed.

2.1-2 Top-Bottom Contact OTFT

Step1. Substrate and gate electrode

4-inch n-type heavily-doped single crystal silicon wafer (100) is used as the substrate and the gate electrode.

Step2. Gate oxide formation

After the initial RCA cleaning, the 1000Å thermally grown SiO2 layer is deposited in furnace.

Step3. Au deposition for Bottom Contact

The bottom electrode is Au. The step forms the Bottom-Contact in OTFT and the one-side (bottom-side) contact in Top-Bottom Contact OTFT. Au provide a better injection by ULVAC thermal coater at deposition pressure 3×10^{-6} torr. The thicknesses of the Au layer are 500~1500Å. We use shadow mask to define bottom contact of each device.

Step4. Pentacene film deposition through shadow mask

Pentacene, which was obtained form Aldrich Chemical Company without any purification, was used as an active layer. The deposition is started at a pressure lower than 3×10^{-6} torr. The deposition rate is controlled at 0.5Å/s. The temperature we use in

depositing pentacene films is 70 $^{\circ}$C. We use shadow mask to define the active region

of each device.

Step5. Au, Al deposition for Top Contact

The step forms the Top-Contact in OTFT and the one-side (top-side) contact in

Top-Bottom Contact OTFT. The top electrodes are Au or Al. Au or Al is deposited on

the active layer by ULVAC thermal coater at deposition pressure 3×10^{-6}torr. The

thicknesses of the metal layer are 500Å. We use shadow mask to define top contact of

each device.

2.2 Measurement Methods and Parameters extraction

We measured all the device characteristics in the darks at room temperature. In this TBC series of experiments, we compare devices with channel length in different structures. The channel width is 600μm and length is 25~800μm in TBC OTFT, TC OTFT and BC OTFT. We provide the drain voltage from 0 to -30V and change the gate voltage from 0 to -30V, step by -6V. The I_D-V_D curves show the turn-on operation of the device. In transfer characteristics (I_D-V_G), the gate bias ranged from 20 to -40V, and the drain voltage (-3V to -30V) are provided for the device with 1000Å film. From the transfer characteristics data, we can extract the mobility and threshold voltage from the square-root of drain current and transconductance.

In the Vertical OTFT, when the drain bias is applied on electrode A, the output characteristics are defined as Group-A characteristics. When the drain bias is applied on electrode B, the output characteristics are defined as Group-B characteristics.

In this parameters extraction section, we introduce the methods for the extraction of mobility, threshold voltage, and on/off current ratio.

2.2-1 Mobility

Generally, mobility can be extracted from the transconductance g_m in the linear region:

$$g_m = \left[\frac{\partial I_D}{\partial V_G}\right]_{V_D=cons\tan t} = \frac{WC_{OX}}{L}\mu V_D$$

(2.1)

Mobility can also be extracted from the slope of the curve of the square-root of drain current versus gate voltage in the saturation region, i.e. $-V_D > -(V_G - V_{TH})$:

$$\sqrt{I_D} = \sqrt{\frac{W}{2L}\mu C_{OX}}(V_G - V_{TH}) \qquad (2.2)$$

2.2-2 Threshold voltage

Threshold voltage is related to the operation voltage and the power consumptions of an OTFT. Many researches on OTFTs are suffered from the large threshold voltage. Threshold voltage is influenced by the ratio of the mobile and trapped carriers at the interface between the organic semiconductor layer and insulator. There are also researches on lowering the threshold voltage by adjusting the insulator layer [30]. In our experiments, we extract the threshold voltage from equation (2.2), the intersection point of the square-root of drain current versus gate voltage when the device is in saturation mode operation.

2.2-3 On/Off current ratio

Devices with high on/off current ratio represent large turn-on current and small off current. It determines the gray-level switching of the LCD displays. High on/off current ratio means there are enough turn-on current to drive the pixel and sufficiently low off current when the device is turned off.

2.2-4 Contact resistance

There are several issues affecting the performance of OTFTs. The air-stability of the organic film is bad, the quality of the organic film is not well-controlled, and the injection is limited by barrier between the source/drain contact and the channel. Hence, the contact resistance is important and serious in OTFTs [31,32].

In the operation of OTFT devices, the gate bias is provided to open the channel for carriers, and the drain bias is used to direct and guide the carrier transportation. The path from the source to the drain can be represented as a circuit with loaded resistances.

The choice of the contact materials is related to the injection efficiency. If the work function of the electrode is not close to the HOMO or LUMO level, there will be a potential barrier formed at the interface. High work function metals such as Au,

Pt, and Pd are preferred to provide better injection efficiency, and the contact will be Ohmic-like.

In the linear operation region of OTFTs for small drain voltage and large gate voltage, the ratio of the drain voltage and drain current represents the total resistance R_{ON}. From equation (1.3), we can obtain

$$R_{ON} = R_{CH} + R_C = (\frac{\partial I_D}{\partial V_D})^{-1} = \frac{L}{W} \frac{1}{\mu C_{OX}} \frac{1}{V_G - V_{TH}} + R_C \tag{2.3}$$

The total resistance in transport path can be divided into channel resistance R_{CH} and contact resistance R_C. The contact resistance is independent of the channel length. Therefore, as we take the relationship between the total resistance and the channel length as shown in Fig. 2.6, the contact resistance can be extracted from the R_{ON} versus L curve when the length equals zero. The drain voltage from -1 to -5V and the gate bias with V_{G1}, V_{G2}, V_{G3}, and V_{G4} are provided. When the gate bias is larger, the barrier between the contact and the semiconductor layer is lowered and the injection of carriers gets better.

.

Chapter 3

Experiments Results and Discussion

## 3.1 Vertical OTFTs (VOTFTs)

To enhance organic transistor performance, the most popular method is the reduction of the transistor channel length[7]. With the high-resolution lithography systems, such as G-Line, I-Line system, or the e-beam direct writer system, the organic devices with nano-scale channel length can be realized[8]-[10]. However, organic electronics will be used in large area and low-cost applications in the future. Proposed new-OTFT architecture should be conformed to the goal of the practical application and the mass production.
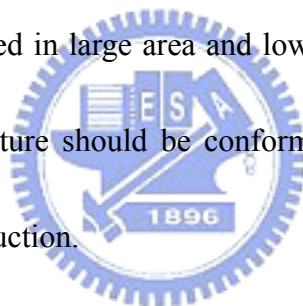
Vertical OTFT is a short channel OTFTs, which is fabricated by a simple process. Without complex architecture, but by stacking the metal and the organic thin films, it is relatively easy to achieve through low-resolute shadow-mask and photolithography process. In VOTFTs, channel length was determined by the organic film thickness and reducible from hundreds of micro meter (~100μm) to nano meter (~100nm). VOTFTs intend increasing more current and gaining better electronic characteristics in the short channel device. Firstly, the output characteristics of the Group-A VOTFT (as defined in experiment) are shown in Fig. 3.1. It is obviously that the

unsaturated drain-current was observed.   This is similar to previous reports on the

short channel organic [33] or a-Si TFT [34].   In Fig. 3.2, the transfer characteristics

were plotted in semi-logarithm scale.   With the increasing of drain bias, the larger

the on/off current ratio is achieved.

In contrary, the Group-B devices were exhibited different properties.   In Fig. 3.3,

a well saturated drain-current could be obtained under high drain-bias.   The behavior

was similar to the traditional long-channel organic transistors.   Compared Group-A,

the transfer characteristics had higher turn-on current and higher on/off current ratio

in low-voltage operation.
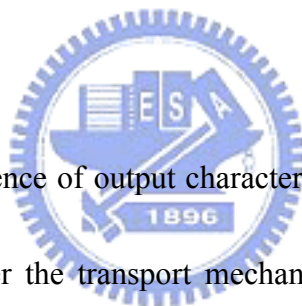
To further study the difference of output characteristics between the Group-A and

Group-B devices, we consider the transport mechanism in these VOTFTs.   It had

been well accepted and verified that the transports in OTFTs strongly affected by 2

distinct mechanisms.   One is the carrier injection through the barrier, which is

built-up at the metal/organic interface.   The other one is the multiple trapping and

re-exiciting mechanisms when the carrier transport inside the organic film.   For

Group-B devices, the electrode pads were separated and the distance between source

and drain electrode was about 200μm.   Thus, when carriers traveled in the pentacene

film, the transporting-path was followed the lateral distance from the source to the

drain electrodes.   Since the distance (channel length) and the output characteristics

(saturated drain current) were similar to conventional OTFTs. According to Zyung's [35] and Leufgen's [36] studies, the saturation drain current may originate from pentacene with gate control but not dominated by contact properties in organic devices…

On the other hand, as for Group-A devices, the vertically configured metal pad were overlapped. The carriers injected from source to drain electrode inside the pentacene layer should travel through a very short distance (<100nm). Whereas the transporting-path in the pentacene film was relatively short and the electric field between the source/drain was vary large. Devices characteristic was no more dominated by the organic film and the other effect should be reconsidered in Group-A devices. Thus, the contact properties were introduced to describe the output characteristics. It is suggested that when the thin pentacene film was bias under high electric field, the field-assisted transporting may influence the carrier transport [37, 38].

A tunneling mechanism: "Approximated Fowler-Nordheim transport" was proposed in short-channel pentacene-OTFTs [33]. The transport described the injection between the metal/organic film were explained by the following equation:

$$I_D \propto F \cdot e^{\frac{-F_0}{F}}$$

Where $F=|V_D/L|$, V_D is the drain bias, L is the channel length and F_0 is a

barrier-related constant. If the Fowler-Nordheim transport is the dominant

mechanism, a linear-relationship can be found in the $ln(I_D/V_D)$ v.s. $1/|V_D|$ plot under

high electric field. In Fig. 3.5(a) and 3.5(b), we show the $ln(I_D/V_D)$ v.s. $1/|V_D|$ plot

for Group-A devices and Group-B devices, respectively. As it is observed, a good

linear relationship can be fitted well with Group-A devices. For Group-B devices,

no obvious dependence can be found. This comparison clearly demonstrates that the

Group-A devices and Group-B devices exhibit different carrier transport mechanism.

This could give an reasonable explain for their different behavior in the output

characteristics.

Since the vertical devices with ultra-short channel length (Group A devices)

exhibited Forwler-Nordheim-like transport. For improving the device performance,

increasing the gate control ability could be a practical way [14].

Therefore, we tried to modify the source/electrode pad to improve the gate

control-force. Based on MOSFET theory, the gate controlling ability could adjust

hole density in the interface between the insulator and the active region. Thus, if we

could increase the transport-channel and the gate controlling ability, the VOTFTs

performance could be enhanced. Therefore, the non-overlap region of re-configured

source/drain pad should be increased. The meshed-like source electrode was then

designed and illustrated in Fig. 2.3. The output characteristics of this new device are

shown in Fig. 3.6. It is found that the devices could be operated under lower drain or gate voltage. From the transfer characteristics depicted in Fig. 3.7, the obvious improvement can be found by comparing to those in Fig. 3.2. The on/off current ratio was significantly increased from $\sim 10^2$ to $\sim 10^4$ orders and the drain and gate voltages were both reduced from more than 20V to less than 10V. The results showed the meshed-like electrode was an effective way to improve the controlling ability for VOTFTs.

3.2 Top-bottom Contact OTFT (TBC OTFT)

The other architectures are the Top-Bottom-Contact OTFTs. The Top-Bottom-Contact OTFTs are viewed as modified VOTFTs but the source/drain electrodes are not overlapped. As shown in Fig. 3.8 (a)-(b), two kinds of Top-Bottom-Contact OTFTs are demonstrated. In Fig.3.8 (a), the bottom electrode is served as the source-electrode and the top electrode is served as drain-electrode. In Fig.3.8 (b), the bottom electrode is served as the drain-electrode and the top electrode is served as source-electrode. These configurations are named as named as TBC bottom-source and TBC top-source OTFTs, respectively.

Respectively, Fig. 3.9 (a) and (b) are the output and transfer characteristics of TBC-bottom-source. According to the I_D vs. V_D curves, the TBC-bottom-source showed the conventional long-channel OTFTs characteristics. The output current is tended to saturate under high drain voltage. In the previous result [39], the Top-contact OTFTs show better performance than the Bottom-contact OTFTs. To further characterize the TBC-bottom-source performance. Fig. 3.11 presents the field effect mobility of three distinct OTFT configurations (TBC-bottom-source, Top-contact, and Bottom-contact). The field effect mobility was plotted as the function of channel length. Evidently, the field effect mobility of TBC-bottom-source OTFTs is higher than the bottom-contact OTFTs, but lower than the Top-contact OTFTs. Generally, the contact resistance is a dominated factor that

influences the extracted mobility and the performance of OTFTs. Thus, to study a

novel OTFT configuration, constructing the resistance model is necessary.

Since the current path through an OTFT was composed with series of resistances.

The total resistance R_{total} can be presented as:

$$R_{total} = \frac{\partial V_D}{\partial I_D} = R_s + R_{channel} = R_s + \frac{L}{W\mu C_{ox}(V_G - V_{th})}$$

Where V_{DS} the drain voltage, I_D is the drain current, Rs is the parasitic resistance,

Rchannel is the channel resistance, L is channel length, W is the channel width, μ is

the field mobility C_{ox} is the capacitance per unit area, V_G is the gate-voltage, V_{TH} is the

threshold voltage. As presents in the equation, the channel resistance is a function of

channel length and gate-voltage. Thereby, we can obtain the parasitic resistance and

the channel resistance by plotting the total resistance as a function of channel length.
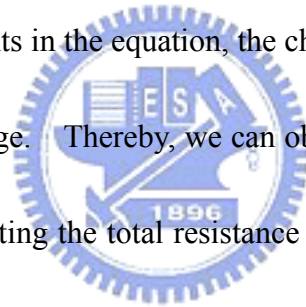
Then, the parasitic resistance is extracted from the intercept and the channel resistance

is calculated from the slope of the straight line.

The conventional method applied a simple model to analyze the transistor

resistances. But in the real case of the OTFT, the parasitic resistance and the channel

resistance should be separated into several detail parts. The contact between the

metal/organic films is not a perfect Ohmic-contact; it usually shows the rectified

properties. The contact can not penetrate into the organic film overall; its finite

thickness between the current path and the metal contact will contribute an additional

resistance.   Usually, the organic film quality degrades seriously near or on the metal

contact.   The degradation will also introduce an uncertain resistance.

Here, we proposed a new assumption.   The series of resistance in the current path

may be defined as four parts.   The first is the contact resistance between the metal

pad and the organic film, the magnitude is independent of channel length and gate

voltage.   The second is the film resistance; it is a function of device channel length

and the gate voltage.   The third resistance is defined as vertical resistance, which is

connected between the channel resistance and the contact resistance in Top-contact

OTFTs.   Finally is the Schottky resistance.   The resistance describes the injection

limitation on the source pad of the Bottom-contact OTFTs.   It is neither a function of

channel length and the gate voltage.   The Schottky resistance also presents the

additional resistance originating from the organic film that degrades near or on the

metal contact.   The assumption is illustrated in Fig. 3.12 (a).

To verify the model, the new constructed resistance was extracted from

conventional architecture: Top-contact OTFT and Bottom-contact OTFT.   All the

resistances in the Top-contact OTFTs are described as:

$$R_{total} = 2 \cdot R_{ct} + 2 \cdot R_{vt} + R_{ft}$$

Where the R_{ct} is the contact resistance between the organic/metal interfaces, the R_{vt} is

the vertical resistance, and the R_{ft} is the film resistance.   In Top-Contact OTFTs, the

total resistances were plotted as a function of channel length.   As shown in Fig 3.13,

under several gate-voltages biasing (V_G=-18V, -24V, -30V), all the straight line will

intersect at the same point (corresponding to the x-axis at –delta l).   The

corresponding magnitude of the y-axis (R_{total}) is the sum of the two contact resistances

in the Top-contact OTFTs.   The vertical resistance is extracted from the condition of

"zero" channel length.   Each vertical resistance (under different gate-voltage); is

defined as the intersect value of each strain line and the total resistance minus the two

contact resistances.   Finally, the film resistance is defined as the total resistance

minus the two contact resistances and the two vertical resistances.   The extracted

resistances plotted as the function of gate-voltages are also shown in Fig 3.14.
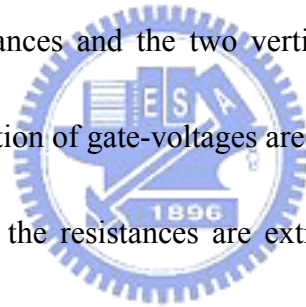
In Bottom-contact OTFTs, the resistances are extracted by the identical method.

The total resistance is defined as:

$$R_{total} = 2 \cdot R_{cb} + R_{cs} + R_{bt}$$

The R_{cb} is the contact resistance between the metal/organic interfaces. But at the

injection contact (source electrode), which is not set as a Ohmic-contact.   An

additional resistance, Schottky resistance; like the additional injection limitation, is

only connected with the source electrode.   Similarly, the film resistance is defined as

the total resistance minus the two contact resistances and the Schottky resistances.

The illustration of the modeling assumption and the extracted resistance was plotted

as a function of the gate-voltage in Fig. 3.15 and Fig. 3.16.   In the Fig. 3.17, two film

resistances from the Top-contact OTFTs and the Bottom-contact OTFTs are presented

as the function of gate-voltage.   The two OTFTs were all fabricated from the same

run.   Thus, the film (pentacene) resistances should be identical.   In Fig. 3.17, the

film resistances are approached under different gate-voltage biasing.   The result is

agreed with the assumption.

   To examine the transport of the TBC bottom-source OTFTs, the model is illustrated

in Fig. 3.18 (a).   In TBC bottom-source, similar to the Bottom-contact OTFTs, the

carrier injected from the source electrode should be suffered an injection barrier.   On

the other side, the contact is identical to the Top-contact OTFT.   The architecture

should be viewed as the hybrid-OTFT, which is combined with the modeling of

Top-contact OTFTs and Bottom-contact OTFTs.   Thus, the total resistance may be

described as:

$$R_{total} = R_{cb} + R_{cs} + R_{ft} + R_{vt} + R_{ct}$$

The total resistance from the modeling and the experiment are plotted in Fig. 3.19 (a);

as the function of gate-voltage.   Evidently, the modeling prediction is good agreed

with the experimental result.

   In the TBC-top-source OTFTs, the injection electrode (source) is identical to the

Top-contact OTFTs.   The injected carriers will not suffer the Schottky-like barrier.

The total resistance may be also described as:

$$R_{total} = R_{cb} + R_{ft} + R_{vt} + R_{ct}$$

The total resistance from the modeling and the experiment are plotted in Fig 3.18 (b) and 3.19 (b); as the function of gate-voltage. Evidently, the modeling prediction is also good agreed with the experimental result.

Chapter 4

Conclusion

In this investigation, the novel vertical organic thin film transistors (VOTFTs) and the Top-bottom-contact OTFTs (TBC OTFTs) were proposed. With the metal shadow-mask and the simple photolithography, the short channel (channel length less than 100nm) OTFTs with vertical structure was fabricated. As well as the common short channel transistors, the unsaturated drain current (under high drain-voltage) was observed in the proposed VOTFTs. It is found that the Fowler-Nordheim tunneling dominated the carrier transport in VOTFTs, resulting in the unsaturated drain-current. To further improve the VOTFTs performance, the modified meshed-source pad was proposed. The control of the gate bias was enhanced and the drain voltage can be significantly reduced. The modified VOTFTs can be operated at low drain-voltage and low gate-voltage (about -5V) and the on/off current ratio was also increased from 10^2 orders to 10^4 orders. The Top-bottom-contact OTFTs was also fabricated by the metal shadow-mask. It is found that the TBC OTFTs performance is between he Top-contact and the Bottom-contact OTFTs. To investigate the transport model of the proposed TBC OTFTs, the series resistance analysis is introduced. The total resistance of the TBC OTFTs was composed of the contact resistances, the vertical resistance, the film resistance, and the barrier limitation of Schottky resistance from

the Top-contact and the Bottom-contact OTFTs.　Comparing the modeling result to

the experimental evidence, a good agreement is observed under different gat-voltage.

References

[1] H. Shirakawa, E. J. Louis, A. G. MacDiarmid, C. K. Chiang, and A. Heeger, "Synthesis of electrically conducting organic polymers: Halogen derivatives of polyacetylene, (CH)x", J. Chem. Soc. Chem. Commun, Vol. 00, pp. 578, (1977)

[2] A. Tsumura, K. Koezuka, and T. Ando, "Macromolecular electronic devices: Field-effect transistor with a polythiophene thin film", Appl. Phys. Lett. Vol.49, pp. 1210, (1986)

[3] F. Ebisawa, T. Kurosawa, S. Nara, "Electrical properties of Polycaetylene/polysiloxane interface", J. Appl. Phys, Vol. 54, pp. 3255-3259, (1983)

[4] R. Smith, D. Allee, C. Moyer, and D, Loy, "Flexible Transistor Arrays", SID 21, 18, (2005)

[5] C. D. Dimitrakopoulos, D. J. Mascaro, "Organic thin-film transistors: a review of recent advances", IBM J. Res. Dev 45, 11-27, (2001)

[6] C. Reese, M. Roberts, Mang-mang Ling, and Z. Bao, "Organic thin film transistors", Materialstoday, Vol. 7, pp. 20-27, (2004)

[7] C.W. Chu, S.H. Li, C.W. Chen, V. Shrotriya, Y. Yang, "High-performance organic thin-film transistors with metal oxide/metal bilayer electrode" , Applied Physics Letters, Vol. 87, pp.193508, (2005)

[8] K. Puntambekar, J. Dong, G. Haugstad, C.D. Frisbie, "Structural and electrostatic complexity at a pentacene/insulator interface" , Adv. Funct. Mater, Vol.16, pp.679 (2006)

[9] M. Kawasaki, S. Imazeki, M. Ando, Y. Sekiguchi, S. Hirota, "High-resolution full-color LCD driven by OTFTs using novel passivation film", IEEE Transactions on Electron Devices, Vol. 53, pp. 435- 441, (2006)

[10] K. Tsukagoshi, J. Tanabe, I. Yagi, K. Shigeto, "Organic light-emitting diode driven by organic thin film transistor on plastic substrates", Journal of Applied Physics, Vol. 99, pp.064506

[11] Z. Bao, A. Dodabalapur, A. J. Lovinger, "Soluble and processable regioregular poly(3-hexylthiophene) for thin film field-effect transistor applications with high mobility" Appl. Phys. Lett. Vol. 69, pp.4108, (1996)

[12] Y.Y. Lin, D. J. Gundlach, S. Nelson, T. N. Jackson, "Stacked pentacene layer organic thin-film transistors with improved characteristics", IEEE Electron Device Lett, Vol. 18, pp.606, (1997).

[13] G. M. Wang, J. Swensen, D. Moses, and A. J. Heeger, "Increased mobility from regioregular poly (3-hexylthiophene) field-effect transistors", J. Appl. Phys, Vol

93, pp 6137, (2003)

[14] L. Sebastian, G. Weiser, and H. Bassler, "Charge transfer transitions in solid tetracene and pentacene studied by electroabsorption", Chemical Physics, Vol 61, pp 125-135, (1981)

[15] E. A. Silinsh, and V.Capek, "Organic Molecular Crystals: Their Electronic States ", New York, (1980)

[16] Y. S. Yang, S. H. Kim, J. Lee, H.Y. Chu, L. Do, "Deep-level defect characteristics in pentacene organic thin films", Applied Physics Letters, Vol. 80, pp. 1595-1597, (2002)

[17] H. Yanagisawa, T. Tamaki, M. Nakamura, K. Kudo, "Structural and electrical characterization of pentacene films on SiO2 grown by molecular beam" Thin Solid Films, Vol. 464-465, pp.398, (2004)

[18] D. Knipp, R. A. Street, A. Vö̈ lkel, J. Ho. "Pentacene thin film transistors on inorganic dielectrics: Morphology, structural properties, and electronic transport" Journal of Applied Physics, Vol. 93, pp.247, (2003)

[19] C. D. Dimitrakopoulos, J. Kymissis, S. Purushothaman, (Proceedings of The Int. Conf. on Digital Printing Technologies, NIP16, Society of Imaging Science and Technology, Vancouver 2000), pp. 493.

[20] N. Tessler, Y. Roichman, "Two-dimensional simulation of polymer field-effect transistor", Appl. Phys. Lett, Vol. 79, pp.2987, (2001)

[21] N.J. Watkins, L. Yan, Y. Gao, "Electronic structure symmetry of interfaces between pentacene and metals", Appl. Phys. Lett, Vol. 80, pp.4384 (2002)

[22] H. Sirringhaus, N. Tessler, R. H. Friend, "Integrated Optoelectronic Circuits Based on Conjugated Polymers", Science, Vol. 280, pp.1741, (1998)

[23] H. Sirringhaus, N. Tessler, R. H. Friend, "Integrated, high-mobility polymer field-effect transistors driving polymer light-emitting diodes", Synth. Met, Vol. 102, pp.857, (1999)

[24] Z. Bao, Y. Feng, A. Dodabalapur, V. R. Raju, A. J. Lovinger, "High Performance Organic Transistors Fabricated by Printing Techniques", Chem.Mater, Vol. 9, pp.1299, (1997)

[25] T. Torsi, "Novel applications of organic based thin film transistors", Solid-State Elecronics, Vol 45, pp 1479-1485, (2001)

[26] P. Parashkov, E. Becker, S. Hartmann, G. Ginev, D. Schneider, H. Krautwald, T.Dobbertin, D. Metzdorf, "Vertical channel all-organic thin-film transistors", Appl. Phys. Lett, Vol. 82, pp.4579 (2003)

[27] M.L. Chabinyc, J.P. Lu, R.A. Street, Y. Wu, P. Liu, B.S. Ong, "Short channel effects in regioregular poly(thiophene) thin film transistors", J. Apply. Phys, Vol. 96, pp.2063 (2004)

[28] T. Oyamada, H. Sasabe, C. Adachi, S. Okuyama, N. Shimoji, K. Matsushige, "Electroluminescence of 2,4-bis(4-(2ʳ-thiophene-yl)phenyl)thiophene in organic light-emitting field-effect transistors", Appl. Phys. Lett, Vol. 86, pp.093505 (2005)

[29] M. D. Austin, S.Y. Chou, "Fabrication of 70 nm channel length polymer organic thin-film transistors using nanoimprint", Appl. Phys. Lett, Vol. 81, pp.4431 (2002)

[30] M. Halik, H. Klauk, U. Zscieschang, G. Shmid, C. Dehm, M. Schutz, S. Maisch, F. Effecberger, M. Brunnbauer, and F. Stellacci, "Low-voltage organic transistors with an amorphous molecular gate dielectric",Nature, Vol 43, pp 963-966, (2005)

[31] H. Klauk, G. Schmid, W. Radlik, W. Weber, L. Zhou, C. D. Sheraw, J. A. Nichols, T. N. Jackson, "Contract resistance in organic thin film transistors", Solid States Electronics, Vol 47, pp 297, (2003)

[32] N. Yoneya, M. Noda, N. Hirai, K. Nomoto, M. Wada, and J. Kasahara, "Reduction of contact resistance in pentacene thin-film transistors by direct carrier injection into a-few-molecular-layer channel", Appl. Phys. Lett, Vol 85, pp 4663, (2004)

[33] Y. Chen, W.W. Zhu, S Xiao, I. Shih, "Fabrication of short channel organic thin film transistors by Si-etching method", J. Vac. Sci. Technol. Vol. A22, pp.768 (2004)

[34] I. Chan, A. Nathan, "100-nm Channel Length a-Si: H Vertical Thin Film Transistors", Amorphous and Nanocrystalline Silicon Science and Technology (MRS Spring Meeting, San Francisco), pp.643, (2004)

[35] T. Zyung, S.H. Kim, H.Y. Chu, J.H. Lee, S.C. Lim, J.I. Lee "Flexible organic LED and organic thin-film transistor", Proceedings of the IEEE (Future Technol. Div., Electron. & Telecommun. Res. Inst., Daejeon, South Korea), Vol. 93, pp.1265, (2005)

[36] M. Leufgen,, U. Bass, T. Muck, T. Borzenko, G. Schmidt, J. Geurts, V. Wagner, L.W. Molenkamp, "Optimized sub-micron organic thin-film transistors: the influence of contacts and oxide thickness" , Synthetic metals, Vol. 146, p.341, (2004)

[37] J. Collet, O. Tharaud, A. Chapoton, D. Vuillaume, "Low-voltage, 30 nm channel length, organic transistors with a self-assembled monolayer as gate insulating films (a-6T)", Appl. Phys. Lett, Vol. 76, pp.1941 ,(2000)

[38] L. Wang, D. Fine, T. Jung, D. Basu, H.V. Seggern, A. Dodabalapur, "Pentacene field-effect transistors with sub-10-nm channel lengths", Appl. Phys. Lett, Vol. 85, pp.1772, (2004)

[39] "A High-Performance Short-Channel Bottom-Contact OTFT and Its Application to AM-TN-LCD", K. Nomoto, N. Hirai, N. Yoneya, N. Kawashima, M. Noda,